

UNLIMITED

Trans 2189

2

AD-A239 057



ROYAL AEROSPACE ESTABLISHMENT

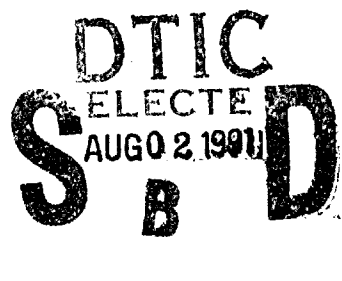
Library Translation 2189

January 1991

Theoretical Study of the Flow in a Rotating Duct.
Experimental Study Through Flow Visualisation
in a Curved Duct

by

Joel Guidez
Pierre-Jaques Michard
Denis Dutoya
Jean Perucchini



DISTRIBUTION STATEMENT A

Approved for public release;
Distribution Unlimited

Procurement Executive, Ministry of Defence
Farnborough, Hampshire

UNLIMITED

91-06659



UNLIMITED

ROYAL AEROSPACE ESTABLISHMENT

Library Translation 2189

Received for printing 29 January 1991

**THEORETICAL STUDY OF THE FLOW IN A ROTATING DUCT.
EXPERIMENTAL STUDY THROUGH FLOW VISUALISATION
IN A CURVED DUCT**

[ÉTUDE THEORIQUE DE L'ÉCOULEMENT DANS UN CANAL EN ROTATION.
APPROCHE EXPERIMENTALE PAR LA VISUALISATION DE
L'ÉCOULEMENT DANS UN CANAL COURBE]

by

Joel Guidez
Pierre-Jacques Michard
Denis Dutoya
Jean Perucchini

Office National d'Etudes et de Recherches Aérospatiales, Chatillon

AGARD-CP-469 (1989)

Translated by

J.D. Southon

Translation Editor

S.P. Harasgama

SUMMARY

An experimental and theoretical study of heat transfer and flow in a rotating duct is under development at ONERA. The duct simulates in a simplified manner an internal cooling passage of the blade of a turbine rotor.

It has been experimentally demonstrated that the rotational velocity causes an increase in thermal exchange by convection in the duct. This phenomenon is explained by secondary flows due to Coriolis force.

The theoretical aspect of the work involves the solution of the Navier-Stokes equations in three dimensions (time marching, ADI method). For both laminar and turbulent flows, the results obtained demonstrate the significance of secondary structures (having both two and four vortices).

Also, by using a rotation-curvature analogy, visualisation of the flow with air or hydrogen bubbles in a water duct gives rise to the same flow structures.

UNLIMITED

LIST OF CONTENTS

	Page
1 INTRODUCTION	3
2 GENERAL	3
3 THERMAL MEASUREMENTS	5
4 NUMERICAL SOLUTION OF THE NAVIER-STOKES EQUATIONS FOR A ROTATING DUCT	7
5 VISUALISATION OF FLOW LINES IN A CURVED DUCT	9
6 CONCLUSION	11
Acknowledgments	12
List of Symbols	13
References	15
Discussion	17
Illustrations	Figures 1-12



Accession For	
NTIS GRA&I	<input checked="" type="checkbox"/>
DTIC TAB	<input type="checkbox"/>
Unannounced	<input type="checkbox"/>
Justification	
By	
Distribution	
Availability Codes	
Dist	Avail and/or Special
A-1	

1 INTRODUCTION

Experimental work has been conducted at ONERA¹, with the aim of studying the influence of the effects of rotation on convective heat transfer within the internal cavities of turbine rotor blades. This work, in common with that carried out with other experimental installations²⁻⁴, in which the axis of the duct under consideration is perpendicular to the axis of rotation, illustrates the differences in the convective exchanges compared with those obtained in a static duct.

These differences are related to secondary flows caused by Coriolis forces, also to the effect of buoyancy close to the walls, which is for the most part due to the centrifugal force.

In parallel with this experimental approach, there has been a theoretical one in hand which employs the numerical modelling of flow in a rotating duct. This approach involves the solution of the Navier-Stokes equations in three dimensions. A number of programs have been compiled. The first of these can accommodate only simple shapes and may be regarded as a preliminary stage of development. In a second stage, effort has been directed towards a more general program, which is being validated. The interesting feature of this program, apart from predicting the effects of rotation in a duct of simple shape, will be the representation of flow and heat transfer in the actual internal cavities of rotor blades (Fig 1)⁵. This implies the simulation of effects associated with large curvatures (Fig 2) or disturbances related to "turbulence initiators" (ribs, webs, pin-fins, Fig 3) with or without rotation.

2 GENERAL

As pointed out in the Introduction, the internal cavities of modern turbine blades are of complex shape. This complexity is related to the pursuit of an artificial increase in the turbulence of the flow by means of shape (successive curves, turbulence initiators) to lead to an enhancement in convective exchange.

The rotation of the rotor blades adds to the effect of the shape.

Although the combined study of complex shape and rotation is of practical interest, it does not allow the separate effects to be readily distinguished. The normal approach is to study each of the phenomena independently before combining them.

Furthermore, the prediction of these turbulent flows ($10000 \leq Re_{DH} \leq 60000$), which can be carried out only by the solution of the Navier-Stokes

equations in three dimensions, requires these programs to be validated with the model of turbulence employed. The latter approach becomes progressively complex.

As a first step therefore, the chosen shapes will be straight ducts with rectangular sections.

In Fig 4, a simplified internal cooling passage of a turbine blade is shown, together with the Coriolis and centrifugal forces caused by rotation. Two straight "centrifugal" and "centripetal" ducts are joined by a curved section. The experimental results demonstrate a significant change in the transfer of convective heat with rotational velocity¹⁻⁴. An overall increase in convective heat exchange as a result of local effects is observed; an increase along the pressure faces of the internal duct, and a reduction along the suction faces.

These changes in heat transfer with rotational velocity are explained by the effects of secondary flow associated with Coriolis force and also buoyancy, which becomes more significant with temperature difference between the wall and the flow.

The secondary flows in particular are responsible for a distortion of the velocity profiles, compared with those obtained in a static duct, and therefore also of the differences in coefficients of friction. The resulting local variations in the exchange coefficients, associated with mixing of the flow, lead to an overall increase in heat transfer.

The equations governing the flow of a compressible fluid in a straight duct are given below for a system of axes relative to the duct (Fig 5). They include terms relating to centrifugal force ($\rho\omega^2x$, $\rho\omega^2y$) and Coriolis force ($2\rho\omega v$ and $-2\rho\omega u$)⁶.

We have equations of:

continuity

$$\frac{\partial \rho}{\partial t} + \nabla \cdot (\rho \underline{v}) = 0 ,$$

motion

$$\frac{\partial}{\partial t} (\rho \underline{v}) + \nabla \cdot (\rho \underline{v} \underline{v} + p \underline{I} - \underline{\tau}) = \rho \Omega^2 \underline{x} + 2\rho \underline{v} \wedge \underline{\Omega} ,$$

energy

$$\frac{\partial}{\partial t} (\rho E) + \nabla \cdot (\rho \underline{v} E + \underline{v} p - \underline{v} \cdot \underline{\underline{I}} + \underline{g}) = \rho \Omega^2 \underline{\pi} \cdot \underline{v} ,$$

$\underline{\Omega}$ = vector rotation (0, 0, ω)

$\underline{\pi}$ = radius (x, y, 0)

\underline{v} = velocity vector (relative) (u, v, w)

$\underline{\underline{I}}$ = tensor variable

$\underline{\underline{I}}$ = frictional constraint tensor

\underline{g} = heat flux vector

In the dimensional analysis the following non-dimensional quantities are significant:

Nusselt	$Nu = hD_H/k$	characterising the heat transfer
Reynolds	$Re = \rho \bar{u} D_H / \mu$	characterising the flow turbulence
Rossby	$Ro = \omega D_H / \bar{u}$	characterising the Coriolis aspect
Ekman	$Ek = Re \cdot Ro = \rho \omega D_H^2 / \mu$	characterising the Coriolis aspect
Rayleigh	$Ra = \bar{u}^2 \omega^2 H D_H^3 (T_p - T_{a_i}) \cdot Pr$	characterising the centrifugal aspect.

These quantities are employed in order to group together the results relating to the influence of rotation on the heat transfer.

3 THERMAL MEASUREMENTS

A general view of the test rig is given in Fig 6. Its dimensions and characteristics, as well as the experimental conditions, were chosen to facilitate the taking of measurements. Also, in order to use as simple a technology as possible, the rotational velocity and the temperature of the test models were reduced by comparison with the values met in an actual blade ($\omega_{\max} = 5000$ rev/min and $T_{p_{\max}} = 400^\circ\text{C}$, instead of 13000 rev/min and 1000°C for a rotor blade).

Two similar test models (Figs 7 and 8) are able to turn inside an electric heater ($T_{\text{FOUR}, \max} = 1200^\circ\text{C}$ and $P = 45$ kW). This assembly is placed inside a vacuum chamber (pressure < 20 Pa). Thus the models are externally heated by

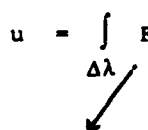
radiation from the electric heater; external convection is negligible on account of the low pressure in the chamber. They are cooled by the circulation of air entering at the bottom of the rotating shaft and leaving at the top; the flow rate, in the range 5-50 g/s, is measured by an ultrasonic flowmeter.

Four sets of rotating seals ensure the absence of leaks in the air supply and the vacuum chamber.

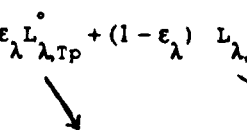
An electric motor drives the shaft supporting the models via a toothed belt.

Measurements are made using thermocouples attached to the various sections (Fig 7). An infrared pyrometer of short time-constant ($\Delta t = 10 \mu s$) and spatial resolution of the order of 1.2 mm allows contours of the radiation temperature to be obtained in a section of the test model⁷. In Fig 8, an example of a contour obtained by pyrometer is given, with a model similar to the cooling passage shown in Fig 4. From two angles of view ($\theta = \pm 45^\circ$) the temperature contour is constructed for two rotational velocities. Distortion of the contour with increase in rotational velocity may be clearly seen. The points c, d, e and f define the boundaries of a section $(x - r_B)/D_H = 9.5$ centrifugal duct, and it is to be noticed that the transfer of heat by convection is greatly increased for the pressure face (the concave surface of the rotor blade), since the wall temperature is less, compared with the case of low rotational velocity ($\omega = 50$ rad/s). On the other hand, for the suction face (the convex surface of the blade) the exchange is less. The significance of the measurements carried out by infrared pyrometry is the direct observation of the thermal effects associated with rotation and, in particular of the Coriolis effect, which gives rise to flow phenomena which are different at the opposing concave and convex faces. The differences noted between the values obtained from the thermocouples may be explained by reflections of the radiation from the heater on to the part of the surface being observed. The output of the pyrometer is of the form:

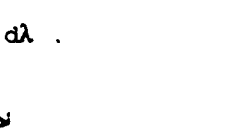
$$u = \int_{\Delta\lambda} F_\lambda \cdot (\epsilon_\lambda L_{\lambda,TP}^\circ + (1 - \epsilon_\lambda) L_{\lambda,env}) d\lambda$$



internal function
of the pyrometer



actual emission
from the surface



reflection from
the surroundings

The exchange coefficients are derived by carrying out a thermal balance at each thermocouple under both transient and steady-state conditions:

$$\rho c_p \frac{dT_p}{dt} = \varepsilon (g_{inc} - \sigma T_p^4) - h(T_p - \bar{T}_o) + g_{cond}.$$

For the centrifugal duct of the model shown in Fig 7, the ratio of the Nusselt number with rotation (Nu_ω) to the Nusselt number in a static condition (Nu_o) is given as a function of the Rossby number which describes the Coriolis aspect. The values correlate quite well with the Rossby number, and as stated above, the convective exchange is increased significantly at the concave face and in this case is decreased to a smaller extent at the convex face. This result is consistent with that obtained by Morris² and Johnson³.

4 NUMERICAL SOLUTION OF THE NAVIER-STOKES EQUATIONS FOR A ROTATING DUCT

The prediction of flows and heat transfers in an internal cooling passage of a rotor blade requires the solution of the Navier-Stokes equations in three dimensions. This modelling must be validated for a certain number of elementary configurations before being used for any shape. The comparison of computation with the experimental results given in section 3 is an example.

Some different programs were developed to solve the equations given by system 1 of section 2. The first ones allowed flow in simple shapes to be dealt with, in this case a rotating straight duct or loop. The principle behind the computation is normal, and comprises a centred finite difference method, based upon a three-dimensional curvilinear orthogonal system, whose conservative nature is assured by the integration of the continuity equations over the elementary volumes associated with each node of the network. These volumes of integration are formed inside the domain of computation from three consecutive points in each direction. In the limits, these imaginary "sliding velocities" are stored, and the continuity equations are integrated over the half-volume associated with the point under consideration, taking account of the limiting conditions through the medium of the wall functions. The spatial discretisation provides a system of $5 N_x N_y N_z$ equations of evolution ($N_{x,y}$ and z = number of points in the network in the different directions), which is integrated in the course of time by a semi-explicit method. The inversion operators are linearised, then factorised in each

direction (by the ADI method), and the computation consists of a series of inversions of tridiagonal matrices by (5×5) blocks⁸.

At the moment effort is directed towards a more general program concerned with both the shape (of any curvilinear network) and the limiting conditions. The technique of integration in time is analogous to that just described. The spatial discretisation employs a method of finite volumes with flux splitting (of the Steger and Warming type⁹) and a diagram decentred at five points.

The principal feature of this program, which was conceived for the prediction of flow in a diesel engine, is the ability to modify the shape at each step in time. With regard to the mesh, a transformation which changes the physical domain of computation into an assembly of parallelepipeds facilitates the application of the method. The limiting conditions are very diverse: they include temperature or flow at areas of the wall, and local injection or suction of the flow. For the accuracy achievable with this program the reader should refer to Refs 10 and 11.

In Fig 9 an example of the results of asymptotic three-dimensional computation in laminar flow is given. The flow conditions are: $Re_{DH} = 1000$; $Ro = 0.125$ and $E_K = 125$. and this computation corresponds to a situation in which x is much greater than a and b . The longitudinal velocity gradients $\partial u / \partial x$ are assumed negligible. The quantity $(1/\rho)(\partial p / \partial x) - \omega^2 x$ is fixed; it is homogeneous over the entire section, and it determines the rate of flow. Fig 9a, which shows a system of two vortices, corresponds to a 40×40 mesh and was obtained after 1000 iterations ($D_H = 10$ mm, $t = 5 \cdot 10^{-5}$ s, $CFL = 80$). Fig 9 shows another case with $Re_{DH} = 500$, $Ro = 0.25$, and $E_K = 125$, the secondary flow structure being changed into a system of four vortices. The intense recirculation of the two supplementary vortices is to be noted. This type of result is in agreement with that obtained by Khesgi and Scriven¹², or Speziale et al¹³.

An example of the results obtained in three dimensions in a rotating loop is given in Fig 10. The $(16 \times 32) \times 96$ mesh represents a duct of rectangular section ($a/b = 2$) comparable to the one investigated and shown in Fig 7. The recirculations and the axial velocity contours are illustrated in Fig 10. They demonstrate the complexity of the flow which in this instance is turbulent: $Re = 40000$, $Ro = 0.06$ and $E_K = 2400$. The inlet conditions are a specified stagnation pressure and enthalpy. Downstream, only the static pressure is specified. Flow is zero at the walls (adiabatic flow).

The results obtained with the simplified computer program (first stage, see above) demonstrate the feasibility of the computation for turbulent conditions. They are encouraging, and the numerical study will be followed by the program under development (second stage), which will then allow a quantitative analysis of the thermal exchanges, using different walls.

5 VISUALISATION OF FLOW LINES IN A CURVED DUCT

An experimental approach to the visualisation of secondary flows in a curved duct was embarked upon. In fact, analysis of the equations of motion demonstrates the similarity of behaviour, with respect to centrifugal effects, of flow in a straight rotating duct and that encountered in a curved duct. In both cases, the trajectories of the particles in a Galilean frame of reference are curved and the phenomena are determined by interaction between the inertial forces due to the curvature and the non-uniformity in flow velocity due to wall friction¹⁴.

The significance of such visualisation is to give prominence to the secondary structures brought into being by this effect, also to throw light on the two- and four-vortex duality, to obtain information on the thickness of the recirculation zones, and hence that of the vortex centres themselves.

In practical terms, the rotation-curvature analogy is achieved by equating the Coriolis and centrifugal accelerations associated with the curvature:

$$2\omega\bar{u} = \frac{\bar{u}^2}{R} \Rightarrow R = \bar{u}^2 / 2\omega,$$

and in terms of the equivalent Rossby number for the curvature:

$$Ro_{\text{courbure}} = D_H / 2R.$$

The air-water analogy is achieved by conserving the Dean number

$$Dn = Re_{DH} \cdot \psi^{\frac{1}{2}} \quad \text{with} \quad \psi = 2R/D_H = 1/Ro_{\text{courbure}}.$$

The values chosen for the experiment described here are (Fig 11):

$$R = 0.12 \text{ m} ; D_H = 40 \text{ mm} ; Re_{DH} = 18000 ; Ro_{courbure} = 0.166 ,$$

with a duct of rectangular section having transparent Altuglass walls, of height $a = 60 \text{ mm}$ and width $b = 30 \text{ mm}$ ($a/b = 2$, Fig 7). These dimensions were chosen so as to allow practical visualisation of the flow using bubbles of air or hydrogen. Hydrogen bubbles are obtained from two grids made up of 0.5 mm diameter wires in a $2 \times 2 \text{ mm}$ mesh; they are spaced 2 mm apart, and have 40 V applied across them. In a vertical position they occupy almost the whole cross-section of the duct. Injection takes place $12.5 \times D_H$ (500 mm) from the curved part.

Illumination of a section 2 mm thick allows the flow lines, and therefore the reconstruction of the secondary flow (Fig 12), to be visualised with equal ease both vertically and horizontally. In the first case the illumination is arranged to follow the curvature of the duct; in the second, it is plane.

In Fig 12.1, the flow is visualised in the region of the upper wall and the circulation is centripetal; the recirculation then follows the inner wall (Fig 12.2). In Fig 12.3 (with horizontal illumination in the middle of the duct) a slight centrifugal effect appears. Along the external wall (Fig 12.4.1) the two centres stand out clearly with an increase in the flow in the upper half and a fall in the other (see also the recirculations in Fig 10). An instability at the external wall in the central area is evident on examining Figs 12.4.1 and 12.4.2. In this separation zone of the two vortices, the flow rises or falls intermittently; this may be explained by the appearance and disappearance of two small supplementary vortices. In Figs 12.1 to 12.4.2 visualisation was achieved by air bubbles and the flow may be considered established at the entrance of the curved duct, as the straight part of rectangular cross-section is 1 m long, ie $25 \times D_H$.

Injection of hydrogen bubbles was employed in order to obtain bubbles of smaller diameter ($d \approx 5/100 \text{ mm}$) than those of air ($d \approx 0.5 \text{ mm}$), and which therefore follow the flow better. There is in fact no noticeable difference in behaviour of the two types of bubbles for flow velocities greater than 0.4 m/s .

However, by inclining the system for generating the hydrogen bubbles by a few degrees, a structure having four vortices became evident (Fig 12.4.3, flow

visualisation near the outside wall)). With a significant angle of inclination (45° in Fig 12.4.4) the structure becomes asymmetrical.

Thus, the natural structure appears to be a two-vortex system; however, a small disturbance can induce a four-vortex system. A more significant disturbance leads to asymmetric circulations. These results are not changed qualitatively when the Reynolds number varies in the range 10000-60000.

In Fig 12.1 it is to be noted that the path of the bubbles makes an angle of about 45° with respect to a tangent to the axis of the duct. For the internal and external faces (Fig 12.2 and 12.4.1) the angle between the horizontal and the path of the bubbles is smaller, 25° and 15° respectively.

These angles become smaller as the Reynolds number increases.

The zones of recirculation are thin and of the order of 5-10% of the hydraulic diameter.

It follows that correct modelling under turbulent conditions in this type of flow may be carried out only by refining the mesh adjacent to the walls.

In conclusion to this section, a question of a purely practical nature arises: what is the effect, where convective exchanges are concerned, of these different structures, ie two-vortex, four-vortex, or asymmetrical?

In fact, in addition to the phenomena described above, entry effects playing a significant part in the development of the secondary structures in actual situations (such as the internal cooling passage of a blade) may appear and render any predictions difficult.

6 CONCLUSION

Knowledge of the flow and heat transfer in the internal ducts of the rotor blades of turbines is necessary in order to optimise the shape of these cavities and obtain the best thermal efficiency.

At ONERA a test rig has been set up to evaluate the influence of the effects of rotation on the convective exchanges in a duct which simulated in a simplified manner an internal cooling passage of the rotor blade of a turbine. Experiments have been carried out using two models comprised of tubes having rectangular sections of ratio 2 and 0.5 respectively between the sides. Using these shapes the coefficients of convective exchange were significantly modified when compared with those encountered using a static duct. When the rotational velocity was increased, the overall convective exchange increased; there was a

significant increase on the pressure face of the duct, and a decrease along the suction face.

These effects may be largely explained by secondary flows induced by Coriolis force.

In parallel with this approach, numerical modelling by solution of the Navier-Stokes equations in three dimensions is under development. The results obtained for laminar flow are in accordance with those published by other authors^{12,13}, and for certain values of Rossby and Ekman numbers recirculations appear with either two or four vortices.

For turbulent flow, a complete three-dimensional modelling of a loop with centrifugal, curved and centripetal ducts has been carried out. The complexity of the secondary flows is very apparent, especially in the curved part; distortion of the axial velocity contours is evident, as predicted, to a considerably less degree than in the laminar mode. This kind of computation will be continued using a Navier-Stokes three-dimensional program undergoing validation, which will allow quantitative analysis of the thermal exchanges with the walls.

Secondary flows which arise in a straight rotating duct may be studied experimentally and more simple in a curved duct by effecting a rotation-curvature analogy. The experimental conditions are defined from a situation which has been analysed on a thermal basis (model $a/b = 2$, $Re_{DH} = 18000$ and $Ro = 0.16$).

The visualisation of the paths of air or hydrogen bubbles in the curved duct, using illumination in different horizontal and vertical planes, demonstrates a system of two vortices. However, a moderate flow disturbance introduced at $12.5 \times D_H$ upstream of the curved duct causes this structure to be changed into a four-vortex system. A greater disturbance gives rise to an asymmetric situation.

These qualitative results agree with the predictions of Soh¹⁶ for laminar flow, in respect of the influence of upstream conditions on secondary structures.

Acknowledgments

The authors express their thanks to DRET (Direction de Recherches et Etudes Techniques) and SNECMA, who provided financial support for the research described in this publication.

List of Symbols

C, C_p	specific heat
D_H	hydraulic diameter
e	wall thickness
E	energy = $C_v T + V^2/2$
E_K	Ekmann number
F_{ce}	centrifugal force
F_{co}	Coriolis force
h	heat exchange coefficient
H	eccentricity = $(r_e + L/2)$
k	thermal conductivity
L_λ	monochromatic radiation
L_λ°	black body radiation
m	mass flow of air
Nu	Nusselt number
P	pressure
Pr	Prandtl number
Pr_t	turbulent Prandtl number
q_{cond}	conduction heat flux
q_{inc}	incident radiation heat flux from heater
r, R	radius
Ra	Rayleigh number
Re	Reynolds number
Ro	Rosby number
\bar{T}	mean temperature
T_a	air temperature
T_{FOUR}	heater temperature
T_p	wall temperature
t	time

u, v, w components of flow velocity

V velocity = $(u^2 + v^2 + w^2)^{1/2}$

x, y, z co-ordinates

Greek symbols

β coefficient of expansion

ϵ emissivity

λ wavelength

μ dynamic viscosity

ν kinematic viscosity

ρ density

σ Stefan's constant

ω rotational speed

Suffixes

o static duct

e entrance of straight duct

i inlet conditions

REFERENCES

- | No. | Author | Title, etc |
|-----|--|---|
| 1 | J. Guidez | Study of the convective heat transfer in rotating coolant channel.
<i>J. of Turbomachinery</i> , Vol.111, pp 43-50 (1989) |
| 2 | W.D. Morris
S.P. Harasgama
B. Salemi | Measurements of turbulent heat transfer on the leading and trailing surfaces of a square duct rotating about an orthogonal axis.
ASME Paper 88-GT-114 (1988) |
| 3 | B.V. Johnson
J.C. Kim
J.H. Wagner | Rotating heat transfer experiments with turbine air foil internal flow passages.
ASME Paper 86-GT-133 (1986) |
| 4 | K.M. Iskakov
V.A. Trushin | The effects of rotation on the heat transfer in radial cooling channels of turbine blades.
<i>Thermal Engineering</i> , No.32 (2) (1985) |
| 5 | B. Dambrine
J.P. Mascarell | Dimensional change in fatigue and creep of turbine blades.
(<i>Dimensionnement en fatigue et fluage des aubes de turbine.</i>)
<i>La Recherche Aéronautique</i> , Vol.1, pp 35-45 (1988) |
| 6 | D.B. Spalding
D. Skiadaressis | Heat transfer in ducts rotating around a perpendicular axis.
6th Int. Heat Transfer Conference, Toronto, Vol.2, pp 91-95 (1978) |
| 7 | M. Charpenel
J. Wilhelm | IR pyrometry for the measurement of temperature of turbine blades.
(<i>Pyrométrie IR pour la mesure de températures d'aubes de turbine.</i>)
AGARD-CP-390, Norway, pp 29.1 to 29.10 (1985) |
| 8 | D. Dutoya | A program for calculating boundary layers and heat transfer along compressor and turbine blades.
T.P. ONERA No.1979-88 and Proceedings of the First Int. Conf. of the Numerical Methods in Thermal Problems, Pineridge Press, Swansea (1979) |

No.	Author	Title, etc
9	J.L. Steger R.F. Warming	Flux vector splitting of the inviscid gasdynamic equation with application to finite difference methods, <i>J. Comput. Phys.</i> , Vol.40, No.2 (1981)
10	M.P. Errera	Numerical prediction of fluid motion in the induction system and the cylinder in reciprocating engines. SAE Paper 870594, Detroit (1987)
11	M.P. Errera J. Labbe A. Jerot	Three-dimensional numerical and experimental analysis of in-cylinder flow in an internal combustion engine. SAE Paper 880106, Detroit (1988)
12	H.S. Khesgi L.E. Scriven	Heat transfer and fluid flow in rotating coolant channels. <i>Physics of Fluids</i> , October 1985 (1985)
13	C.G. Speziale	Numerical study of viscous flow in rotating rectangular ducts. <i>J. Fluid Mechanics</i> , Vol.122 (1982)
14	P. Bradshaw	The analogy between streamline curvature and buoyancy in turbulent shear flow. <i>J. Fluid Mechanics</i> , Vol.36, pp 177-191 (1969)
15	K.N. Ghia U. Ghia C.T. Shin	Study of fully developed incompressible flow in curved ducts, using a multi-grid technique. <i>J. of Fluids Engineering</i> , Vol.109, pp 226-236 (1987)
16	W.Y. Soh	Developing fluid flow in a curved duct of square cross-section and its fully developed dual solutions. <i>J. of Fluid Mechanics</i> , Vol.88 (1988)
17	K.C. Cheng F.P. Yuen	Flow visualisation experiments on secondary flow patterns in an isothermally heated curved pipe. <i>J. of Heat Transfer</i> , Vol.109, pp 55-61 (1987)
18	P. Hile R. Vehrenkamp E.O. Schulz-Dubois	The development and structure of primary and secondary flow in a curved square duct. <i>J. Fluid Mechanics</i> , Vol.151, pp 219-241 (1985)

DISCUSSION

D.K. Hennecke, Technische Hochschule, Darmstadt, Germany:

In your measurements, what kind of velocity distribution in the inlet cross section of the test section did you try to achieve and how did you do it?

Author's reply:

The shape of the inlet part, just before the test section (centrifugal duct) has been chosen with the industrial partner (SNECMA) in order to have a similar shape of the channel before the blade.

Therefore, in order to compute accurately the flow in 3D (and consequently the friction and the heat transfer coefficients within the test section) it is necessary to start the computation near the axis of rotation owing to the Coriolis force which induces secondary flow from the hub.

J. Moore, Virginia Polytechnic Institute, USA

The orientation of your bend is at 90° to that used in our paper. Are you also planning to test different bend orientations?

Author's reply:

With the first test section ($a/b = 2$), the objective was specifically the study of the two channels:

- the centrifugal channel one
- the centripetal channel one.

Therefore, the radius of the curved part which connects the two ducts has been chosen in order to minimise the perturbation of the flow induced by the bend.

But, with the second test section ($a/b = 0.5$) the geometry is close to a real cavity of blade and the orientation of the bend is at 90° by comparison to the first test section and like the one computed in the paper of Mr and Mrs Moore.

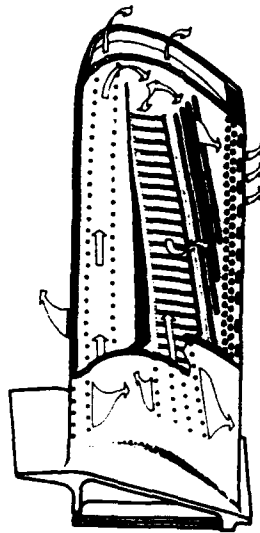


Fig 1 Example of the complex internal cavity of a turbine rotor blade



Fig 2 Example of a simple reversal - visualisation by means of a solution of Teepol and water - $Re_{DH} = 15000$

Figs 3,4&5



Fig 3 Example of a disturbance - duct of square section - visualisation by air bubbles - $Re_{DH} \approx 15000$

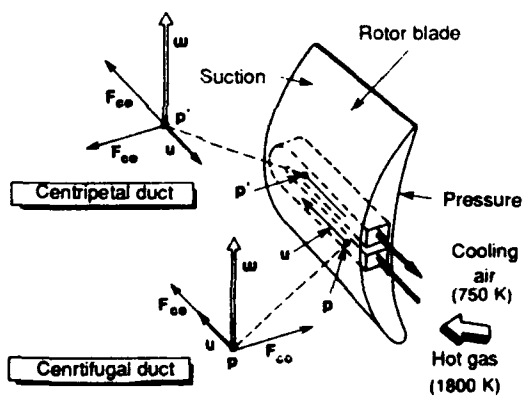


Fig 4 Example of internal cavity

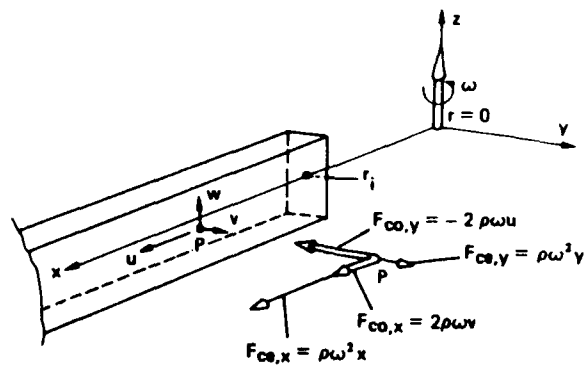


Fig 5 Representation of a straight duct in the rotating axis system

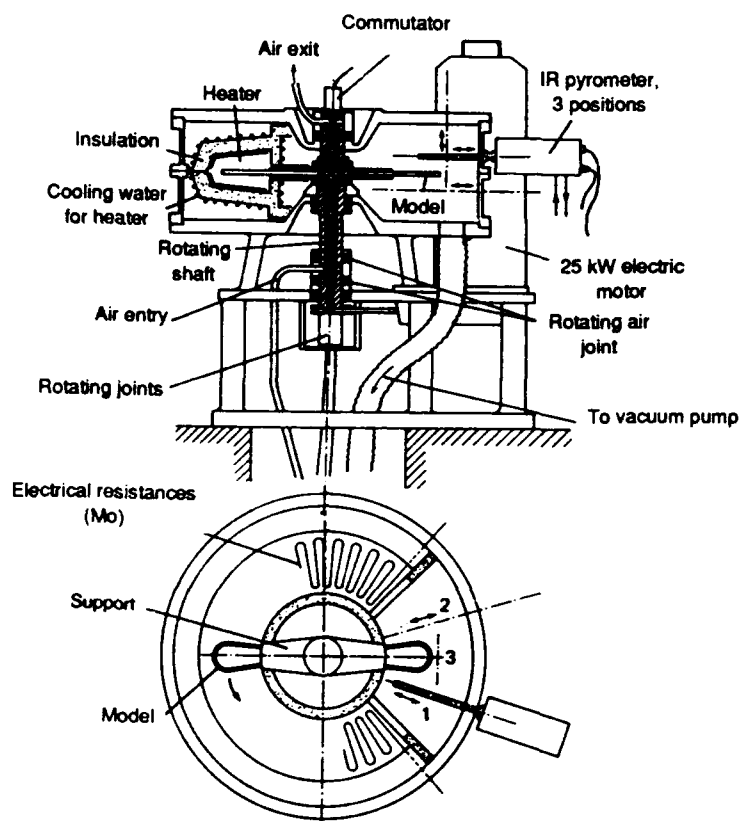
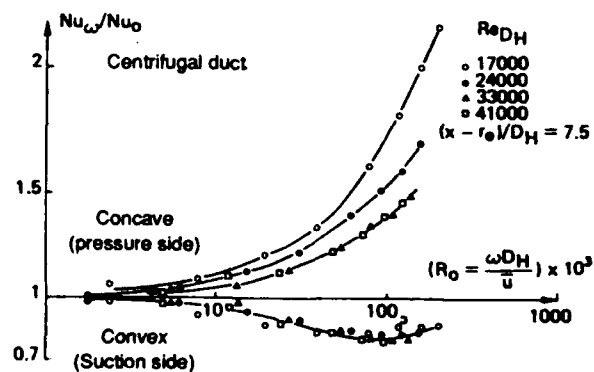
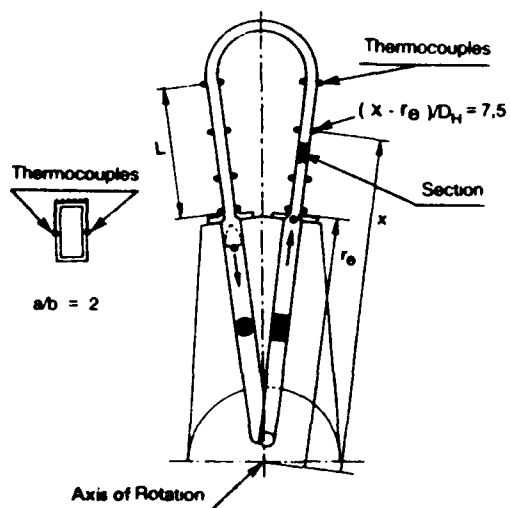


Fig 6 Test rig

Fig 7 Test model $a/b = 2$, and ratio Nu_{ω}/Nu_0 as a function of Rossby number

Figs 8&9

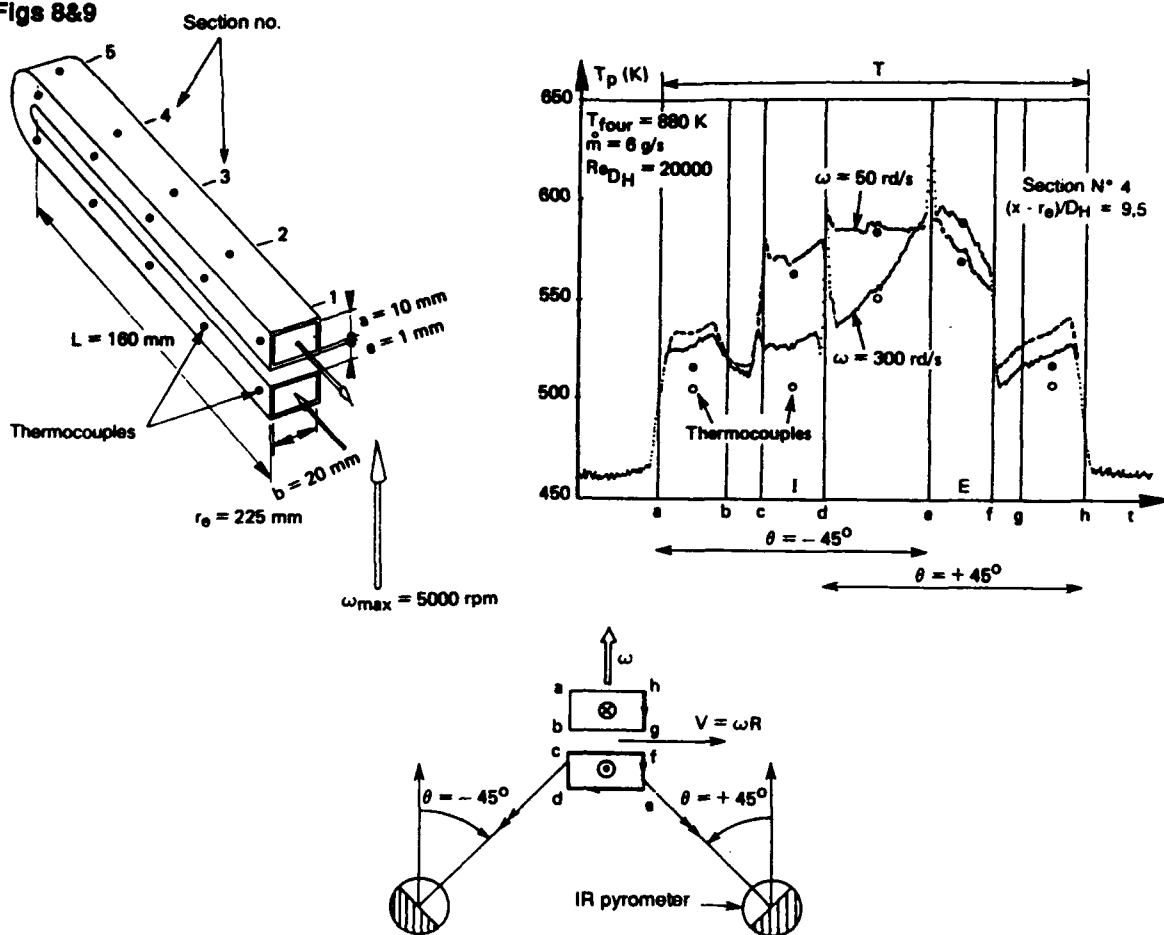


Fig 8 Example of radiation temperature obtained with the IR pyrometer for two rotational speeds $\omega = 50$ and 300 rad/s, model $a/b = 0.5$, $(x - r_e)/D = 9.5$

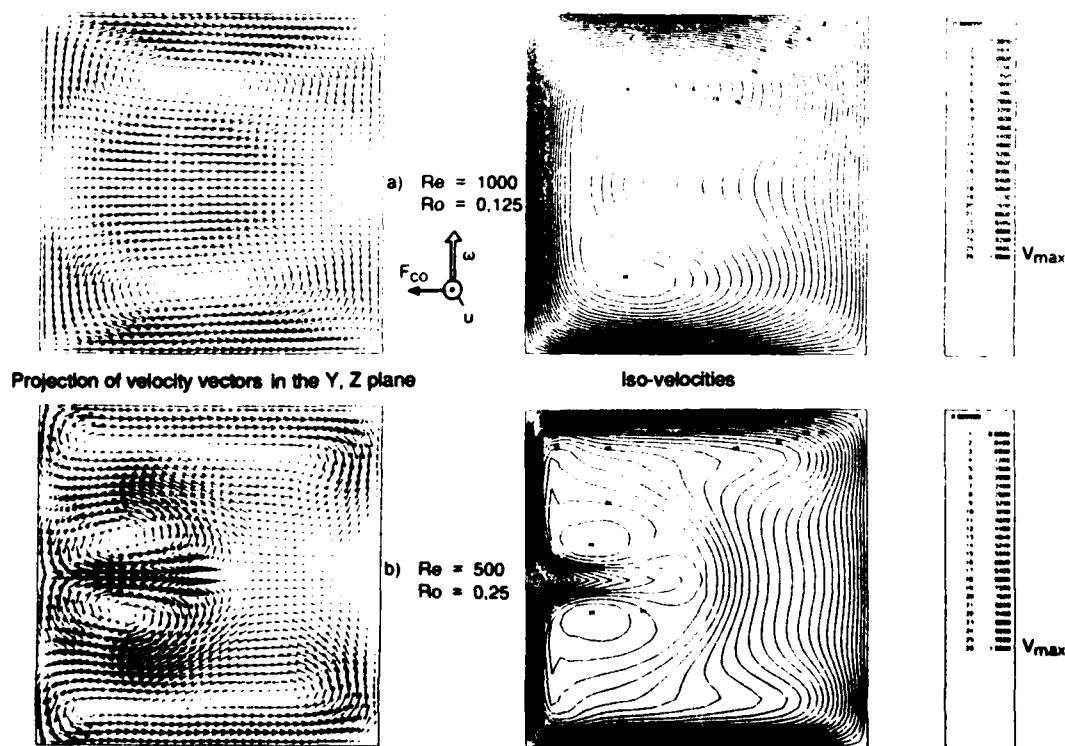


Fig 9 Computations of asymptotic 3D flows (40×40 mesh, $\Delta t = 5.10^{-5}$ s)

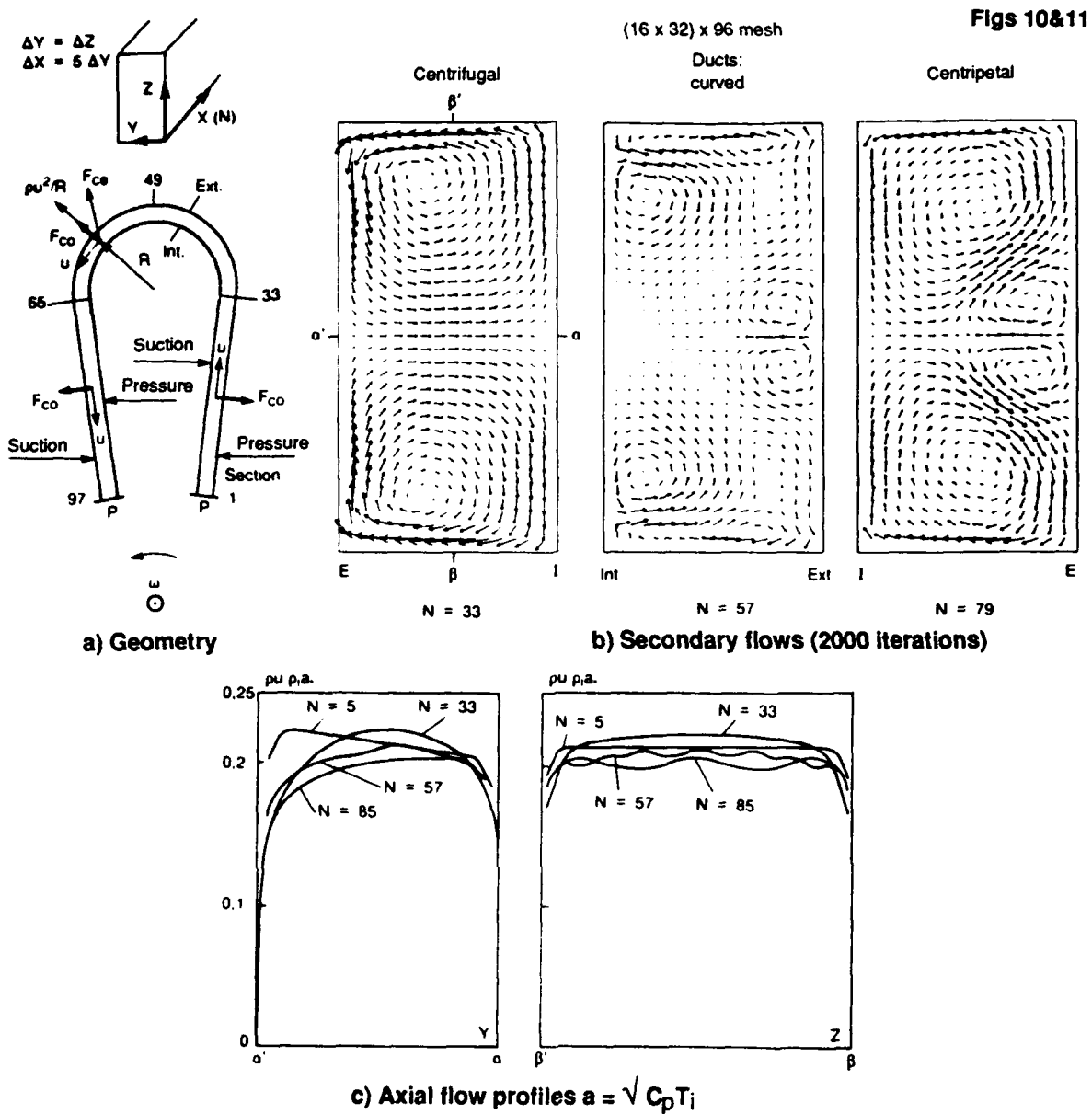


Fig 10 3D computation in a loop - turbulent flow: $Re = 40000$; $Ro = 0.06$

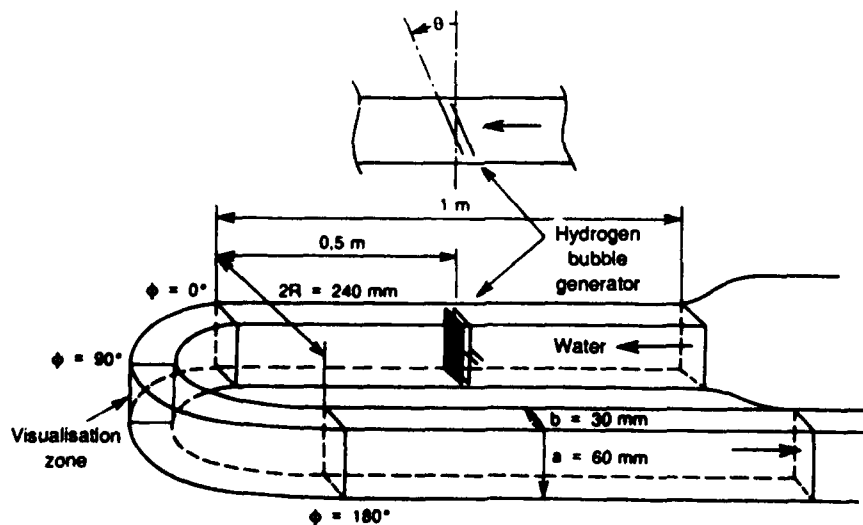


Fig 11 Curved duct: $D_H = 40 \text{ mm}$, $R = 120 \text{ mm}$

Fig 12

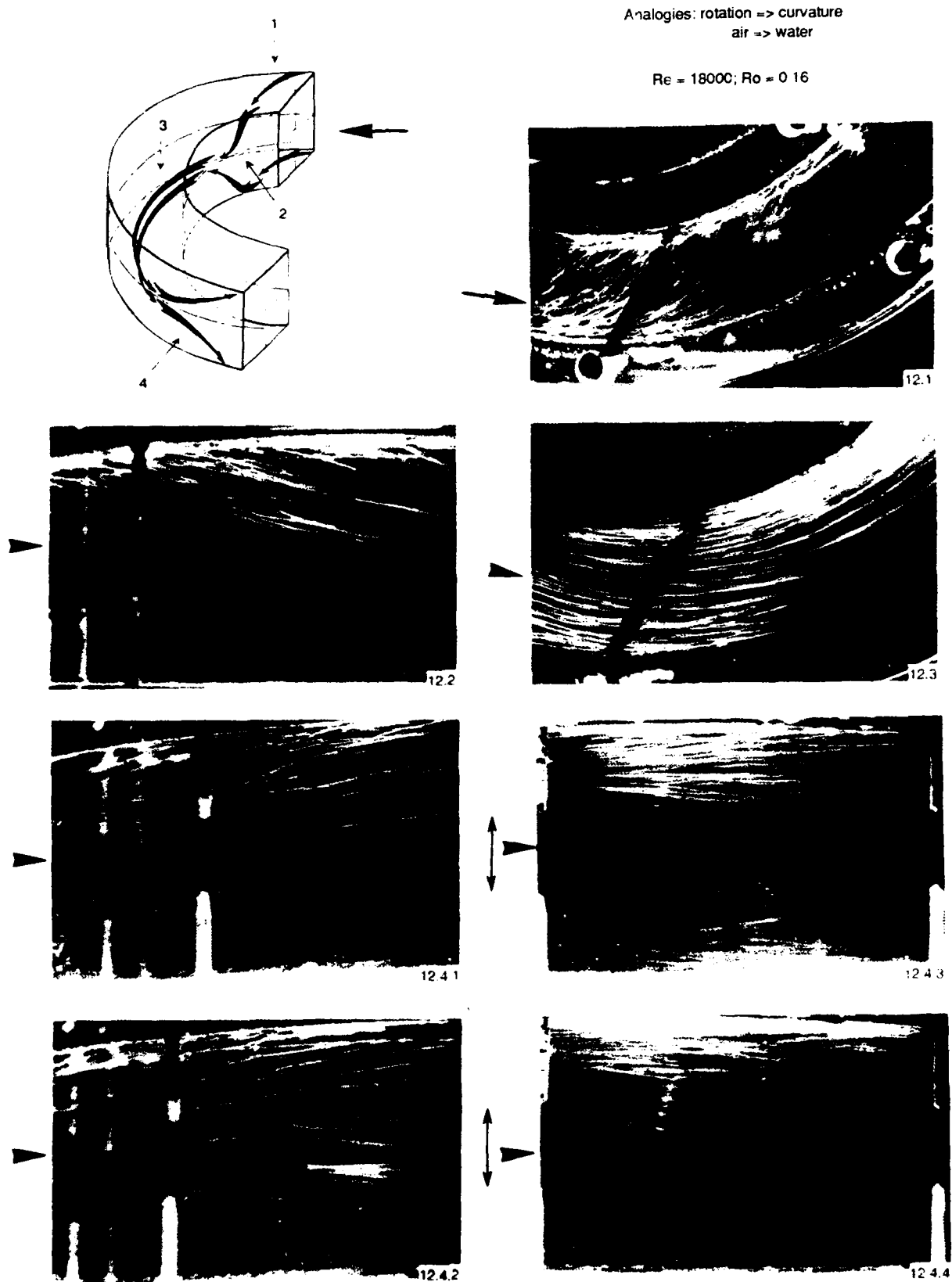


Fig 12 Visualisation of lines of flow in a curved duct